Enhanced structural stability of DNA origami nanostructures by graphene encapsulation

2016 New J. Phys. 18 025016

(http://iopscience.iop.org/1367-2630/18/2/025016)

New Journal of Physics
The open access journal at the forefront of physics

Deutsche Physikalische Gesellschaft DPG
IOP Institute of Physics

Published in partnership with: Deutsche Physikalische Gesellschaft and the Institute of Physics

OPEN ACCESS

RECEIVED
30 November 2015

REVISED
9 January 2016

ACCEPTED FOR PUBLICATION
26 January 2016

PUBLISHED
15 February 2016

PAPER

Enhanced structural stability of DNA origami nanostructures by graphene encapsulation

Aleksandar Matković[1,5], Borislav Vasić[1], Jelena Pešić[1], Julia Prinz[2], Ilko Bald[2,3], Aleksandar R Milosavljević[4,6] and Radoš Gajić[1]

[1] Center for Solid State Physics and New Materials, Institute of Physics, University of Belgrade, Pregrevica 118, 11080 Belgrade, Serbia
[2] Institute of Chemistry—Physical Chemistry, University of Potsdam, Potsdam, Germany
[3] BAM Federal Institute for Materials Research and Testing, Richard-Willsttter Str. 11, D-12489 Berlin, Germany
[4] Laboratory for Atomic Collision Processes, Institute of Physics, University of Belgrade, Pregrevica 118, 11080 Belgrade, Serbia
[5] *Present address*: Institute of Physics, Montanuniversität Leoben, Franz Josef Straße 18, A-8700 Leoben, Austria.
[6] *Present address*: Radiation Laboratory, University of Notre Dame, Notre Dame, IN 46556, USA.

E-mail: bvasic@ipb.ac.rs

Keywords: graphene, DNA origami nanostructures, atomic force microscopy

Abstract

We demonstrate that a single-layer graphene replicates the shape of DNA origami nanostructures very well. It can be employed as a protective layer for the enhancement of structural stability of DNA origami nanostructures. Using the AFM based manipulation, we show that the normal force required to damage graphene encapsulated DNA origami nanostructures is over an order of magnitude greater than for the unprotected ones. In addition, we show that graphene encapsulation offers protection to the DNA origami nanostructures against prolonged exposure to deionized water, and multiple immersions. Through these results we demonstrate that graphene encapsulated DNA origami nanostructures are strong enough to sustain various solution phase processing, lithography and transfer steps, thus extending the limits of DNA-mediated bottom-up fabrication.

1. Introduction

Artificial deoxyribonucleic acid (DNA) macromolecules offer highly controllable bottom-up fabrication of various nanostructures. Since the first demonstration of DNA folding and the wide variety of structures and patterns that can be created at nanoscale [1], many 2D and 3D DNA origami nanostructures were fabricated using this method [2–4]. These structures often serve as substrates [5], offering a solution-based self-assembly with nanometer precision geometries. DNA nanostructures have been used as scaffolds for assembly of metallic nanoparticles [6–8], for routing polymers [9], surface-enhanced Raman scattering [10], as positive and negative masks for DNA nano-lithography [11–14], and even graphene patterning [15].

However, the delicate nature of DNA origami nanostructures constrains their applicability in bottom-up fabrication [16]. In particular any mechanical wear or solution phase processing could damage these nanostructures [7, 17, 18]. Thus enhancing the structural stability of DNA origami nanostructures is crucial for expanding the field of bottom-up nanofabrication.

On the other hand, graphene, a single atomic layer of crystal graphite, with its peerless mechanical properties can offer a solution to this issue. Youngs modulus of graphene is about five times greater than of the bulk steel [19, 20], while at the same time graphene can be folded by 180° over less than one nanometer in length, without breaking its in-plane bonds. The crystal lattice of graphene (and graphite) is so densely packed that it is impermeable to any gases, even H_2 [21]. Also, graphene has low friction coefficient [22], and has been employed as a protective coating for friction reduction [23–27], wear protection [28, 29] and as corrosion barriers [30].

Recently, graphene has been employed to encapsulate objects such as single yeast cells [31], bacteria [32], water molecules [33–42], fluorescent films [43], single-stranded DNA and DNA nanostructures [44, 45]. It was demonstrated that graphene replicates the topography of the DNA molecules [44, 45]. Also, the directed

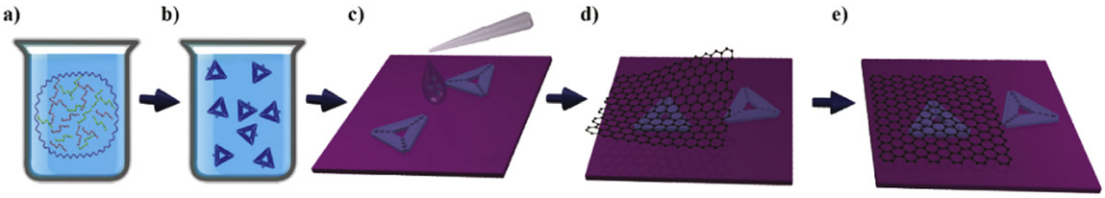

Figure 1. (a) and (b) Schematic representations of DNA origami synthesis; (c) DNA origami deposition; and (d) and (e) encapsulation by exfoliated graphene.

deposition of DNA rectangles onto lithography patterned strips of nitrogen-doped reduced graphene oxide was demonstrated [46].

In this study we focus on enhancing the structural stability of DNA origami nanostructures by graphene encapsulation. For this purpose triangular DNA origami nanostructures are deposited onto silicon substrates and encapsulated by single layer exfoliated graphene. The morphology of DNA origami nanostructures is very well transferred to the graphene, having even the inner triangle clearly resolved by atomic force microscopy (AFM). The samples are tested for their structural stability using AFM based manipulation and aqueous solution exposure. The forces required to damage bare and graphene encapsulated nanostructures are compared, and the effects of cumulative damage introduced by successive manipulations are investigated. In addition, stability of graphene encapsulated DNA origami nanostructures is tested against prolonged exposure to deionized water (DI H_2O).

2. Materials and methods

2.1. DNA origami synthesis

Triangular DNA origami nanostructures were synthesized according to a modified version of Rothemund's method (schematically represented in figures 1(a) and (b)) [1]. Therefore, the M13mp18 virus strand (5 nM, New England Biolabs) serving as scaffold and 208 short staple strands (Integrated DNA Technologies) were mixed in a molar ratio of 1:30 in 1 × TAE (Sigma Aldrich) with 10 mM $MgCl_2$ (total volume 100 μl). The mixture was annealed by gradually decreasing the temperature from 80 °C to 8 °C within 1 h 48 min using a Primus 25 advanced thermal cycler (Peqlab). Excess staple strands were removed by spin filtering the resulting DNA origami solution two times at 3830 g for 10 min using Amicon Ultra-0.5 filters (100 kDa MWCO, Millipore) after the addition of 200 μl (first run) or 300 μl (second run) of 1 × TAE with 10 mM $MgCl_2$.

2.2. DNA origami deposition

After preparation, triangular DNA origami nanostructures were deposited onto ~1 × 1 cm^2 silicon substrates covered with 80 nm thick dry thermal oxide (SiO_2/Si). Due to the interference of the light within the oxide layer, optical contrast of the graphene is enhanced and enables good visibility of graphene using optical microscopy, which is essential for the identification [47].

Before the deposition of DNA origami nanostructures, the substrates were cleaned and prepared by 5 min treatment in Novascan's ozone cleaner. Subsequently, drops of 0.5 μl of DNA origami solution were deposited on each substrate and covered with 10 μl of 10 × TAE with 10 mM of $MgCl_2$. After one hour of incubation period in the water-saturated environment, the samples were rinsed in 1:1 water-ethanol solution to clean excess of material and dried with an argon gun (flow ~10 l min^{-1}). As a result DNA origami nanostructures covered the entire substrates with an averaged density of twenty triangular nanostructures per square micrometer. The DNA origami deposition is schematically represented in figure 1(c).

2.3. Graphene exfoliation

Graphene was deposited using the procedure known as micromechanical cleavage [48], yielding high-quality layers of graphene but limited in lateral size (on the order of tens of micrometers in diameter). Kish graphite (Naturgraphite GmbH) was used as starting material. Graphite flakes were cleaved using sticky tape (Nitto Denko ELP BT150ECM) and deposited on the substrates with DNA origami nanostructures. In order to avoid damaging DNA origami nanostructures, the entire micromechanical exfoliation was carried out at room temperature. After the deposition of graphene on top of the DNA origami nanostructures, individual flakes were detected using optical microscopy and single atomic layer samples were chosen by the optical contrast, and confirmed by the AFM. Schematic representation of the encapsulation by graphene is shown in figures 1(d) and (e).

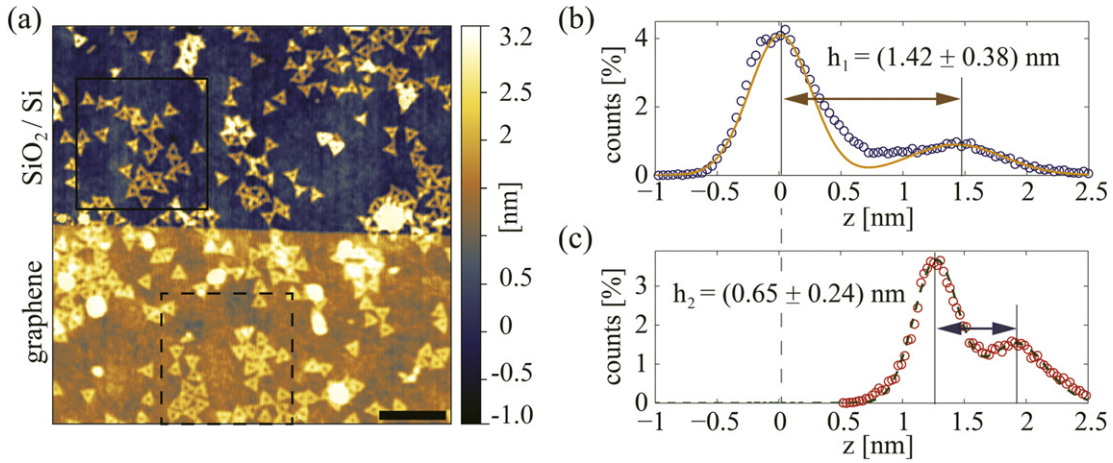

Figure 2. (a) TAFM topography of a step edge of graphene covering a substrate with DNA origami nanostructures. Scale bar is 500 nm. (b) and (c) histograms (circles) and Gaussian fits (solid and dashed lines) of the selected areas in (a), corresponding to the bare and graphene encapsulated nanostructures. h_1 and h_2 stand for the height of the bare and graphene encapsulated structures, and are estimated as a peak-to-peak distance within the corresponding histograms.

2.4. AFM measurements

AFM experiments were carried out on the NT-MDT's NTEGRA Prima system. Imaging before and after AFM manipulation was performed in tapping mode (TAFM), using NSG01 probes from NT-MDT (typical force constant 5.1 N m^{-1}). AFM manipulation was done in contact mode, using NT-MDT's CSG01 probes (typical force constant 0.03 N m^{-1}). All measurements were done at ambient conditions. Initial imaging of the samples was done in TAFM mode. In this mode, the vibrating AFM tip is free from a torsion, so it does not push DNA origami nanostructures laterally leaving them practically intact.

AFM manipulation of graphene has been done using both static [49, 50] and dynamic plowing [51]. Here, AFM manipulation experiments were done in the following way. After selected sample areas were found and visualized using TAFM mode, AFM manipulations were carried out in contact mode, by scanning a selected sample area. Every image was recorded at constant normal force (constant set point). Manipulation on the graphene encapsulated DNA origami nanostructures was carried out using TAFM (NGS01, force constant 5.1 N m^{-1}). However, imaging of bare DNA nanostructures was not possible in contact mode with these hard cantilevers. For this reason the manipulation of bare nanostructures was done using soft CSG01 probes (with two order of magnitude lower force constant).

AFM topography images of the samples were processed in an open source software Gwyddion. For each image first a mean plane was subtracted, followed by line corrections in the scanning direction, and finally a three point plane leveling is applied and the mean height is set to zero value. In the cases of graphene/substrate step edges, the three points were chosen on the bare substrate.

3. Results and discussion

A typical TAFM topography image of a step edge of graphene, with (1.26 ± 0.21) nm height, covering a substrate with DNA origami nanostructures is shown in figure 2(a). In order to estimate the structural damage, both the height and the shapes of the triangular DNA origami nanostructures were considered. The shapes were straightforwardly assessed from the topography images. The height of the structures was determined using a peak-to-peak difference from the selected area histograms, as shown in figures 2(b) and (c). Each histogram peak was fitted by a single Gaussian line. The uncertainty of the measured height was estimated as a half width at half maximum of the histogram peak that corresponds to either bare or graphene encapsulated DNA origami nanostructures. As a result, an average height of the bare triangular DNA origami nanostructures was found to be (1.42 ± 0.38) nm, while the graphene encapsulated ones were (0.65 ± 0.24) nm high. The observed difference is due to non-perfect replication of DNA origami by graphene. Some parts of graphene covering DNA nanostructures do not lie perfectly on SiO_2 substrate. These parts of graphene are slightly lifted above the substrate and make the effective height of the graphene covered DNA nanostructures smaller. This effect is even more pronounced for high density of deposited DNA origami nanostructures since graphene does not fall perfectly on SiO_2 substrate between adjacent DNA nanostructures.

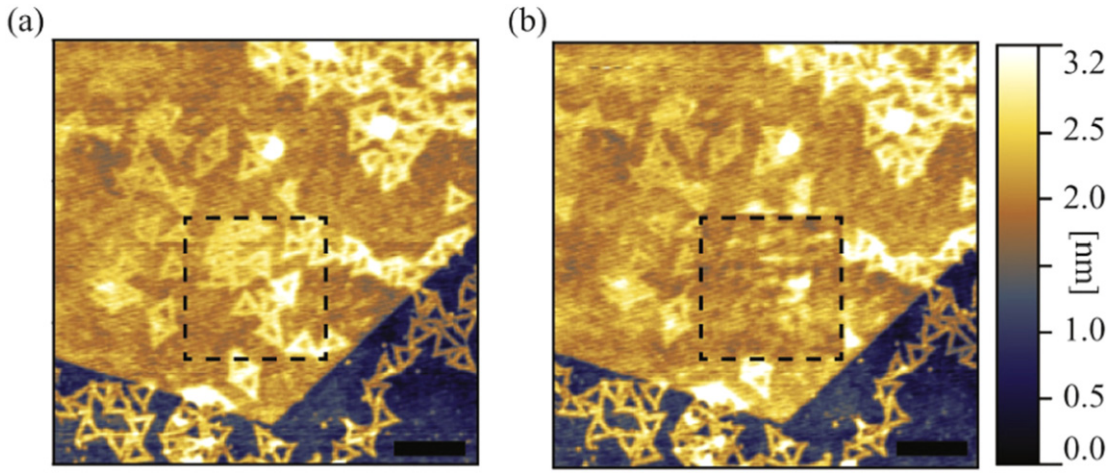

Figure 3. (a) A topography image (TAFM) of DNA origami nanostructures encapsulated by a single layer graphene (top) and on a bare SiO_2/Si substrate (bottom). (b) The same sample area after scanning of the dashed square in contact mode with an applied force up to 76 nN. Scale bars are 250 nm.

3.1. AFM manipulation

Imaging of DNA nanostructures in the contact mode is challenging [44]. Therefore, so far their mechanical properties and stability have been measured using peak force tapping mode with precisely controlled force in pico Newton range [52]. Here AFM manipulation in contact mode was applied in order to determine the forces required to damage both bare and graphene encapsulated DNA origami nanostructures. Figure 3 shows TAFM topography of DNA origami nanostructures before and after manipulation of a 500 $\times$ 500 nm^2 selected area, marked by the dashed square. The selected area was repeatedly scanned six times in contact mode. The applied normal force was increased for each successive scan ranging from 36 to 76 nN. The contact mode topography scans are shown in figures 4(a)–(f). The same probe (NGS01) was used both for the imaging of the sample in TAFM mode and for the manipulation in contact mode. The height of the encapsulated nanostructures was estimated for each contact mode scan using their corresponding histogram peak-to-peak distance. The results are presented in figure 4(g), showing encapsulated structure height as a function of the applied normal force. Both the height and the shape of the triangular origami nanostructures indicate that structural damage starts to occur when a normal force of about 60 nN is exerted.

In order to estimate the amount of mechanical protection that graphene offers to DNA origami nanostructures, the same AFM manipulation experiments are carried out on the bare triangular DNA origami nanostructures (on SiO_2/Si substrate). Here much smaller normal forces are required to damage the structures. Thus, a soft mode probes (CSG01) were used, with the typical force constant of 0.03 N m^{-1}. Figure 5 shows six subsequent scans in contact mode. Again, the normal force is increased for each scan, ranging from 1.8 to 3.1 nN. The triangular DNA origami nanostructures appeared unchanged up to the normal force of 2.5 nN.

The nature of the structural damage that is introduced by the AFM probe is different for the bare and graphene encapsulated DNA origami nanostructures. In the case of the encapsulated nanostructures graphene protects them from attaching to the tip of the AFM probe. As a result, the damaged structures appeared "smudged" and their height is reduced. On the other hand the bare nanostructures tend to attach to the tip and drift in the scanning direction. As a result the height of the bare structures that were not pushed and damaged by the AFM probe does not change significantly (figure 5(f)).

The arrows in figure 5(d) indicate the initial damage of the bare DNA origami nanostructures, that is introduced with the normal force of only 2.7 nN. Compared with the same tests carried out on the encapsulated structures (figure 4), the force required to damage the DNA origami nanostructures is over an order of magnitude greater for the ones encapsulated with graphene. The structural damage that can be introduced by AFM manipulation strongly depends on the adhesion of both the DNA nanostructures and the graphene layer to the substrate. For this reason it is not reliable to set the exact force threshold at which graphene offers wear protection to these structures.

Still the question remains whether the cumulative damage arises when the same graphene encapsulated structures are scanned multiple times. To test this the same graphene encapsulated area was scanned in contact mode ten times successively. The normal force was set to 28 nN for all scans. TAFM topography images of the same sample area before and after manipulation are respectively shown in figures 6(a) and (b). Figure 6(c) shows the height of the graphene encapsulated DNA origami nanostructures for each TAFM and contact mode scan.

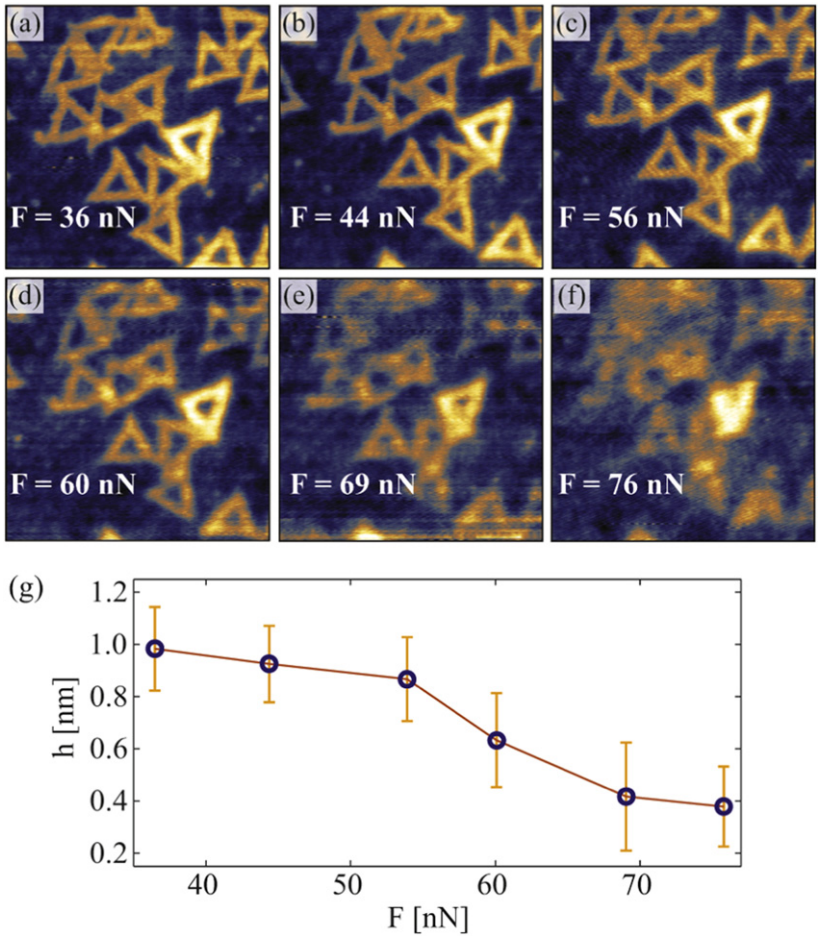

Figure 4. (a)–(f) 500 × 500 nm^2 area of graphene encapsulated DNA origami nanostructures scanned in contact mode with an increase of the applied normal force (set point) for each successive image. The same sample area is also shown in figure 3, and highlighted with the dashed squares. (g) The height of graphene encapsulated DNA origami nanostructures shown in (a)–(f), with respect to the initial values.

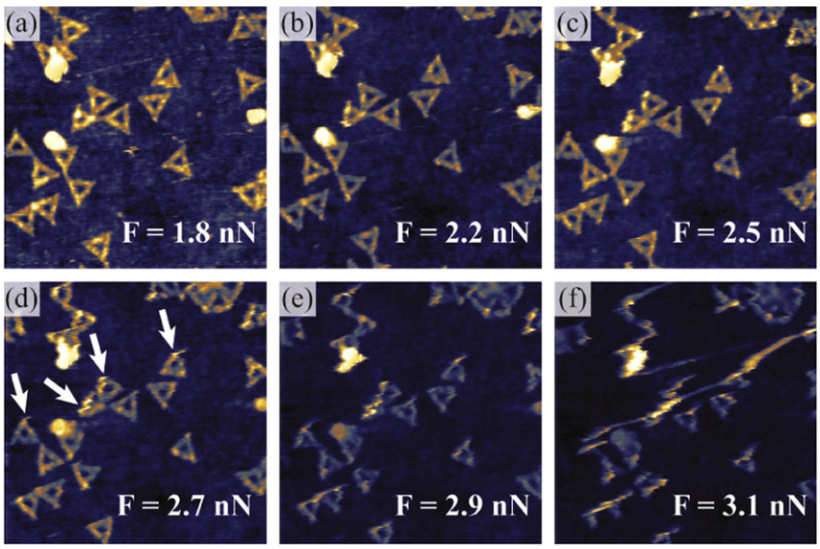

Figure 5. (a)–(f) 1 × 1 μm^2 area of bare DNA origami nanostructures on a SiO_2/Si substrate scanned in contact mode. The applied force (set point) is increased for each successive image. Arrows in (d) indicate the initial damaged areas of the nanostructures, giving a force threshold of about 2.5 nN.

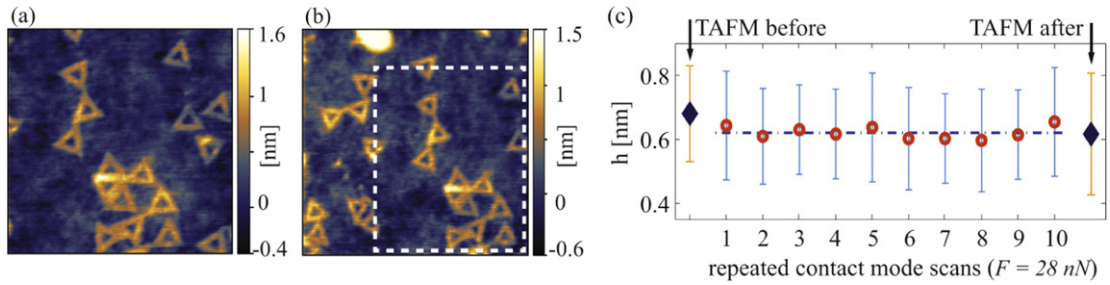

Figure 6. (a) 0.8 × 0.8 μm^2 TAFM topography of graphene encapsulated DNA origami nanostructures prior to multiple scans in contact mode with low applied force ($F = 28$ nN). (b) 1 × 1 μm^2 TAFM topography of the same sample area after ten successive scans in contact mode. The dashed square in (b) indicates the area scanned in contact mode. (c) The height of the graphene encapsulated DNA origami nanostructures after each step. Diamonds indicate TAFM measured height, while circles indicate the height measured in each contact mode scan.

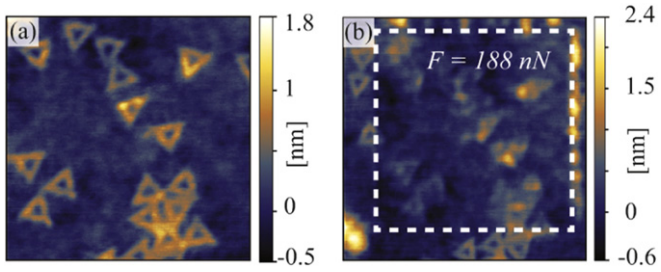

Figure 7. (a) 0.8 × 0.8 μm^2 TAFM topography of graphene encapsulated DNA origami nanostructures prior to a single scan in contact mode with high applied force ($F = 188$ nN). (b) 1 × 1 μm^2 TAFM topography of the same sample area after the scan in contact mode. The dashed square in (b) indicates the area scanned in contact mode.

The heights were obtained as a peak-to-peak distance from their corresponding topography images. The results show that there is no cumulative damage effect if the applied normal force is below the damage threshold (~60 nN).

On the other hand, only a single contact mode scan with high enough force is sufficient to damage graphene encapsulated nanostructures. This is demonstrated in figure 7. Here, TAFM topography images are shown before and after the selected area was scanned in contact mode with the normal force set to 188 nN, well above the damage threshold.

3.2. Deionized water exposure

In order to extend the use of DNA origami nanostructures as scaffolds in the bottom-up nanofabrication [16], these structures need to be strong enough to withstand the harsh conditions needed in many fabrication steps [18]. Commonly these steps include submersion into liquids. Either as the part of the solution phase processing or simple rinsing after a lithography step, DNA origami nanostructures need to withstand both short and prolonged liquid exposures.

In this study the exposure to deionized water was tested on both bare and graphene encapsulated structures. The exposure time was varied between 1 min and 24 h. The SiO_2/Si substrates covered with DNA origami nanostructures and partly encapsulated by graphene were submerged into 10 mL of DI H_2O (Millipore, 18,2 MΩ cm^{-1}) and after the set exposure time quickly dried with an argon gun (flow ~10 l min^{-1}). Water exposure was done successively on each flake, e.g.: the flake was exposed to 1 min in DI H_2O, measured, then again exposed for 4 min more to give the total of 5 min exposure, and so on. This way properties that are unique for every sample, as adhesion of nanostructures and graphene to the substrate, did not figure in the test.

The selected sample areas were imaged using TAFM both prior and after DI H_2O exposure. Figure 8 shows TAFM topography images of triangular DNA origami nanostructures partly encapsulated by graphene before exposure (a) and after various lengths of exposure to DI H_2O (b)–(e).

The unprotected structures are significantly damaged even after only 1 min of DI H_2O exposure, and not lifted-off the substrate. Most likely the amount of residual Mg^{2+} ions on the substrate surface determines whether the structures are damaged or lifted-off the substrate [18].

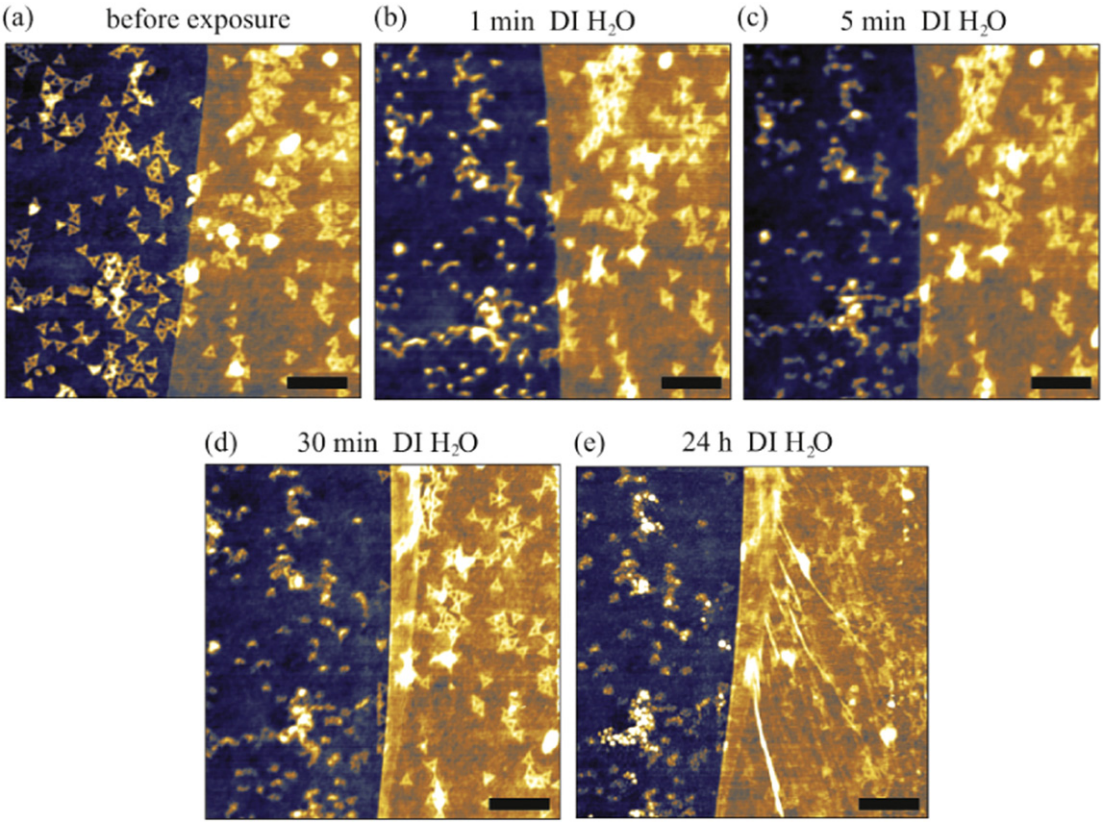

Figure 8. (a) 3 × 3 μm^2 TAFM topography images of an area of graphene encapsulated (right) and bare (left) DNA origami nanostructures, before (a) and after various lengths of exposure to DI H_2O (b)–(e). Scale bars are 500 nm.

Graphene encapsulated DNA origami nanostructures appeared to be intact by the water exposure. Each individual triangular origami was preserved even after 30 min of DI H_2O exposure. The height of the nanostructures was also unchanged. In the case of the sample shown in figures 8(a)–(d) the height of the encapsulated origami nanostructures was 0.8(±0.2) nm, after each exposure. In figure 8(d) the edge of graphene sample was folded, most likely during the drying step.

The only exception occurred after twenty four hours of exposure. In this case graphene started to wrinkle. Although some triangular DNA origami nanostructures are still visible underneath graphene (figure 8(f)), most of the nanostructures were damaged and their height estimation was not reliable.

The exact exposure time threshold will again depend on the adhesion to the substrate of both graphene and DNA origami nanostructures, and varies from sample to sample. Still, very short exposures do damage or lift-off bare DNA nanostructures [18]. On the other hand graphene encapsulation offers significant protection increasing the exposure times by at least two orders of magnitude.

4. Conclusion

In summary, we have demonstrated that single layer exfoliated graphene can be used as a protective layer for DNA origami nanostructures. Through the AFM based manipulation we have shown that the normal force required to damage graphene encapsulated DNA origami nanostructures is over an order of magnitude greater than for the unprotected ones. The threshold for the normal force that induces structural damage to the graphene encapsulated DNA origami nanostructures was found to be about 60 nN. In addition, we have shown that graphene provides wear protection against multiple manipulations if the applied normal force is below the damage threshold.

Besides wear protection, graphene encapsulated DNA origami nanostructures were tested against prolonged exposure to deionized water, and multiple immersions. We show that graphene encapsulated nanostructures remain intact even after 30 min of the exposure to deionized water, while the bare structures are significantly damaged in the matter of seconds. The limits of graphene protection against deionized water exposure arise from wrinkling of the graphene layer itself.

We expect that other liquids will act in the similar manner as long as they do not damage graphene, and will only take different amount of time to damage bare DNA origami nanostructures. This extends the use of DNA origami scaffolds in many fabrication processes, as various lithography steps or wet transfer of 2D materials. Future studies could involve encapsulation by more than one layer of graphene and the use of other 2D materials, as hexagonal boron nitride, which could prove protection in harsh environments that graphene might not be suitable for.

Acknowledgments

This work is supported by the Serbian MPNTR through Projects ON 171005, III 45018, IO 171020, 451-03-2802-IP/1/167, and by the DAAD bilateral project 451-03-01858/2013-09/1 between Republic of Serbia and Germany. BV acknowledges support from COST Action MP1303. IB acknowledges support from a Marie Curie FP7 Integration Grant within the 7th European Union Framework Programme, and by the Deutsche Forschungsgemeinschaft (DFG).

References

[1] Rothemund P W K 2006 Folding DNA to create nanoscale shapes and patterns *Nature* **440** 297–302
[2] Han D, Pal S, Nangreave J, Deng Z, Liu Y and Yan H 2011 DNA origami with complex curvatures in three-dimensional space *Science* **332** 342–6
[3] Ke Y, Ong L L, Shih W M and Yin P 2012 Three-dimensional structures self-assembled from DNA bricks *Science* **338** 1177–83
[4] Wei B, Dai M and Yin P 2012 Complex shapes self-assembled from single-stranded DNA tiles *Nature* **485** 623–6
[5] Bald I and Keller A 2014 Molecular processes studied at a single-molecule level using DNA origami nanostructures and atomic force microscopy *Molecules* **19** 13803–23
[6] Li H, Park S H, Reif J H, LaBean T H and Yan H 2004 DNA-templated self-assembly of protein and nanoparticle linear arrays *J. Am. Chem. Soc.* **126** 418–9
[7] Geng Y, Liu J, Pound E, Gyawali S, Harb J N and Woolley A T 2011 Rapid metallization of lambda DNA and DNA origami using a Pd seeding method *J. Mater. Chem.* **21** 12126–31
[8] Schreiber R, Kempter S, Holler S, Schüller V, Schiffels D, Simmel S S, Nickels P C and Liedl T 2011 DNA origami-templated growth of arbitrarily shaped metal nanoparticles *Small* **7** 1795–9
[9] Knudsen J B *et al* 2015 Routing of individual polymers in designed patterns *Nat. Nanotechnol.* **10** 892–8
[10] Prinz J, Schreiber B, Olejko L, Oertel J, Rackwitz J, Keller A and Bald I 2013 DNA origami substrates for highly sensitive surface-enhanced Raman scattering *J. Phys. Chem. Lett.* **4** 4140–5
[11] Becerril H A and Woolley A T 2007 DNA shadow nanolithography *Small* **3** 1534–8
[12] Deng Z and Mao C 2004 Molecular lithography with DNA nanostructures *Angew. Chem. Int. Ed.* **43** 4068–70
[13] Surwade S P, Zhao S and Liu H 2011 Molecular lithography through DNA-mediated etching and masking of SiO_2 *J. Am. Chem. Soc.* **133** 11868–71
[14] Surwade S P, Zhou F, Wei B, Sun W, Powell A, ODonnell C, Yin P and Liu H 2013 Nanoscale growth and patterning of inorganic oxides using DNA nanostructure templates *J. Am. Chem. Soc.* **135** 6778–81
[15] Jin Z, Sun W, Ke Y, Shih C-J, Paulus G L C, Wang Q H, Mu B, Yin P and Strano M S 2013 Metallized DNA nanolithography for encoding and transferring spatial information for graphene patterning *Nat. Commun.* **4** 1663
[16] Zhang G, Surwade S P, Zhou F and Liu H 2013 DNA nanostructure meets nanofabrication *Chem. Soc. Rev.* **42** 2488–96
[17] Liu J, Geng Y, Pound E, Gyawali S, Ashton J R, Hickey J, Woolley A T and Harb J N 2011 Metallization of branched DNA origami for nanoelectronic circuit fabrication *ACS Nano* **5** 2240–7
[18] Kim H, Surwade S P, Powell A, ODonnell C and Liu H 2014 Stability of DNA origami nanostructure under diverse chemical environments *Chem. Mater.* **26** 5265–73
[19] Lee C, Wei X, Kysar J W and Hone J 2008 Measurement of the elastic properties and intrinsic strength of monolayer graphene *Science* **321** 385–8
[20] Lee G H *et al* 2013 High-strength chemical-vapor-deposited graphene and grain boundaries *Science* **340** 1073–6
[21] Bunch J S, Verbridge S S, Alden J S, van der Zande A M, Parpia J M, Craighead H G and McEuen P L 2008 Impermeable atomic membranes from graphene sheets *Nano Lett.* **8** 2458–62
[22] Kim K-S, Lee H-J, Lee C, Lee S-K, Jang H, Ahn J-H, Kim J-H and Lee H-J 2011 Chemical vapor deposition-grown graphene: the thinnest solid lubricant *ACS Nano* **5** 5107–14
[23] Berman D, Erdemir A and Sumant A V 2014 Graphene: a new emerging lubricant *Mater. Today* **17** 31–42
[24] Klemenz A, Pastewka L, Balakrishna S G, Caron A, Bennewitz R and Moseler M 2014 Atomic scale mechanisms of friction reduction and wear protection by graphene *Nano Lett.* **14** 7145–52
[25] Filleter T, McChesney J L, Bostwick A, Rotenberg E, Emtsev K V, Seyller Th, Horn K and Bennewitz R 2009 Friction and dissipation in epitaxial graphene films *Phys. Rev. Lett.* **102** 086102
[26] Lee C, Li Q, Kalb W, Liu X-Z, Berger H, Carpick R W and Hone J 2010 Frictional characteristics of atomically thin sheets *Science* **328** 76–80
[27] Lee H, Lee N, Seo Y, Eom J and Lee S W 2009 Comparison of frictional forces on graphene and graphite *Nanotechnology* **20** 325701
[28] Berma D, Erdemir A and Sumant A V 2013 Few layer graphene to reduce wear and friction on sliding steel surfaces *Carbon* **54** 454–9
[29] Lin L Y, Kim D-E, Kim W-K and Jun S-C 2011 Friction and wear characteristics of multi-layer graphene films investigated by atomic force microscopy *Surf. Coat. Tech.* **205** 4864–9
[30] Kirkland N T, Schiller T, Medhekar N and Birbilis N 2012 Exploring graphene as a corrosion protection barrier *Corros. Sci.* **56** 1–4
[31] Kempaiah R, Salgado S, Chung W L and Maheshwari V 2011 Graphene as membrane for encapsulation of yeast cells: protective and electrically conducting *Chem. Commun.* **47** 11480–2

[32] Mohanty N, Fahrenholtz M, Nagaraja A, Boyle D and Berry V 2011 Impermeable graphenic encasement of bacteria *Nano Lett.* **11** 1270–5
[33] Xu K, Cao P and Heath J R 2010 Graphene visualizes the first water adlayers on mica at ambient conditions *Science* **329** 1188–91
[34] Cao P, Xu K, Varghese J O and Heath J R 2011 The microscopic structure of adsorbed water on hydrophobic surfaces under ambient conditions *Nano Lett.* **11** 5581–6
[35] Cao P, Xu K, Varghese J O, Xu K and Heath J R 2012 Visualizing local doping effects of individual water clusters on gold(111)-supported graphene *Nano Lett.* **12** 1459–63
[36] Shim J, Lui C H, Ko T Y, Yu Y-J, Kim P, Heinz T F and Ryu S 2012 Water-gated charge doping of graphene induced by mica substrates *Nano Lett.* **12** 648–54
[37] Severin N, Lange P, Sokolov I M and Rabe J P 2012 Reversible dewetting of a molecularly thin fluid water film in a soft graphene-mica slit pore *Nano Lett.* **12** 774–9
[38] He K T, Wood J D, Doidge G P, Pop E and Lyding J W 2012 Scanning tunneling microscopy study and nanomanipulation of graphene-coated water on mica *Nano Lett.* **12** 2665–72
[39] Komurasaki H, Tsukamoto T, Yamazaki K and Ogino T 2012 Layered structures of interfacial water and their effects on Raman spectra in graphene-on-sapphire systems *J. Phys. Chem.* C **116** 10084–9
[40] Lee M J, Choi J S, Kim J-S, Byun I-S, Lee D H, Ryu S and Lee C 2012 Characteristics and effects of diffused water between graphene and a SiO_2 substrate *Nano Res.* **5** 710–7
[41] Li Q, Song J, Besenbacher F and Dong M 2015 Two-dimensional material confined water *Acc. Chem. Res.* **48** 119–27
[42] Song J, Li Q, Wang X, Li J, Zhang S, Kjems J, Besenbacher F and Dong M 2014 Evidence of Stranski–Krastanov growth at the initial stage of atmospheric water condensation *Nat. Commun.* **5** 4837
[43] Lange P, Dorn M, Severin N, Vanden Bout D A and Rabe J P 2011 Single- and double-layer graphenes as ultrabarriers for fluorescent polymer films *J. Phys. Chem.* C **115** 23057–61
[44] Severin N, Dorn M, Kalachev A and Rabe J P 2011 Replication of single macromolecules with graphene *Nano Lett.* **11** 2436–9
[45] Moon Y, Shin J, Seo S, Park J, Dugasani S R, Woo S H, Park T, Park S H and Ahn J R 2014 Nanoscale topographical replication of graphene architecture by artificial DNA nanostructures *Appl. Phys. Lett.* **104** 231904
[46] Yun J M, Im K N, Kim J Y, Shin D O, Lee W J, Lee S H, Lieberman M and Kim S O 2012 DNA origami nanopatterning on chemically modified graphene *Angew. Chem.* **124** 936–9
[47] Blake P, Hill E W, Castro Neto A H, Novoselov K S, Jiang D, Yang R, Booth T J and Geim A K 2007 Making graphene visible *Appl. Phys. Lett.* **91** 063124
[48] Novoselov K S, Geim A K, Morozov S V, Jiang D, Zhang Y, Dubonos S V, Grigorieva I V and Firsov A A 2004 Electric field effect in atomically thin carbon films *Science* **306** 666–9
[49] Giesbers A J M, Zeitler U, Neubeck S, Freitag F, Novoselov K S and Maan J C 2008 Nanolithography and manipulation of graphene using an atomic force microscope *Solid State Commun.* **147** 366–9
[50] Eilers S and Rabe J P 2009 Manipulation of graphene within a scanning force microscope *Phys. Status Solidi* B **246** 2527–9
[51] Vasić B, Kratzer M, Matković A, Nevosad A, Ralević U, Jovanović D, Ganser C, Teichert C and Gajić R 2013 Atomic force microscopy based manipulation of graphene using dynamic plowing lithography *Nanotechnology* **24** 015303
[52] Song J, Zhang Z, Zhang S, Liu L, Li Q, Xie E, Gothelf K V, Besenbacher F and Dong M 2013 Isothermal hybridization kinetics of DNA assembly of two-dimensional DNA origami *Small* **9** 2954–9